Ultrahigh-speed endoscopic optical coherence tomography and angiography enables delineation of lateral margins of endoscopic mucosal resection: a case report

Ther Adv Gastroenterol
2017, Vol. 10(12) 931–936
DOI: 10.1177/1756283X17739503

Ultrahigh-speed endoscopic optical coherence tomography and angiography enables delineation of lateral margins of endoscopic mucosal resection: a case report

Osman O. Ahsen, Hsiang-Chieh Lee, Kaicheng Liang, Zhao Wang, Marisa Figueiredo, Qin Huang, Benjamin Potsaid, Vijaysekhar Jayaraman, James G. Fujimoto and Hiroshi Mashimo

Introduction

Endoscopic mucosal resection (EMR) is a common technique for resecting dysplastic lesions in Barrett's esophagus (BE), stomach, and colon,[1] but precise delineation of dysplastic margins before resection and verification of complete removal after resection remain challenging.[2,3] Endoscopic optical coherence tomography (OCT) enables three-dimensional visualization of tissue microstructure and is commercially available as Volumetric Laser Endomicroscopy (NinePoint Medical, Bedford, MA, USA).[4,5] We recently developed an ultrahigh-speed endoscopic OCT system which operates more than 10 times faster than commercial instruments, generating volumetric images with higher transverse resolution and voxel density.[6,7] This allows visualization of depth-resolved *en face* mucosal and microvascular patterns (OCT angiography [OCTA]), in addition to cross-sections. A recent study with 32 patients reported 94% sensitivity and 69% specificity for identifying dysplasia on blinded assessment of OCTA images.[8] This current report demonstrates the clinical utility of probe-based, ultrahigh-speed endoscopic OCT and OCTA for assessing a dysplastic lesion at the gastroesophageal junction (GEJ), its lateral margins before and immediately after EMR, and at 2-month follow up.

Case presentation and methods

This study was conducted under protocols at the VA Boston Healthcare System Institutional Review Board (IRB), Harvard Medical School Office of Human Research Administration, and Massachusetts Institute of Technology Committee on the Use of Humans as Experimental Subjects. Written informed consent was obtained prior to imaging allowing presentation of this case and data. A 75-year-old man was scheduled for endoscopic eradication therapy of known BE with confirmed high-grade dysplasia (HGD) at the GEJ. The patient had a C0M5 BE segment[9] and no prior endoscopic treatment. Endoscopic OCT and OCTA images were acquired before and immediately after EMR. The patient was imaged again at 2-month follow up. The OCT probe was introduced through the accessory channel of a dual-channel endoscope (GIF-2TH180, Olympus, Tokyo, Japan) to allow co-registered imaging during EMR (Duette® Multiband Mucosectomy, Cook Medical, Bloomington, IN, USA). Each OCT/OCTA dataset covered an area of 10 mm × 16 mm (circumferential × longitudinal), and was acquired in 8 s.[6] Multiple acquisitions were performed by varying probe placement around the lesion and resection margins.

Results

White light endoscopy (WLE)/narrow band imaging (NBI) images prior to EMR showed a dysplastic lesion with nodularity and irregular mucosal and microvascular patterns located at the GEJ within a sliding hiatal hernia (inset, Figure 1a). OCT/OCTA images acquired prior to EMR showed the lesion and its lateral margins (Figure 1). In the *en face* OCT image at 250 μm depth, the gastric/nondysplastic BE (NDBE) region was identified by regular circular mucosal patterns (Figure 1a). The adjacent dysplastic lesion exhibited irregular mucosal patterns. In the *en face* OCTA image at 250 μm depth, the gastric/NDBE region was identified by regular honeycomb

Correspondence to:
James G. Fujimoto
Massachusetts Institute of Technology, 77 Massachusetts Avenue 36-361, Cambridge, MA 02139, USA
jgfuji@mit.edu

Osman O. Ahsen
Hsiang-Chieh Lee
Kaicheng Liang
Zhao Wang
Massachusetts Institute of Technology, Cambridge, MA, USA

Marisa Figueiredo
VA Boston Healthcare System, West Roxbury, MA, USA

Qin Huang
VA Boston Healthcare System, West Roxbury, MA, and Harvard Medical School, Boston, MA, USA

Benjamin Potsaid
Massachusetts Institute of Technology, Cambridge, MA, and Thorlabs, Inc., Newton, NJ, USA

Vijaysekhar Jayaraman
Praevium Research, Inc., Santa Barbara, CA, USA

Hiroshi Mashimo
VA Boston Healthcare System, West Roxbury, MA, and Harvard Medical School, Boston, MA, USA

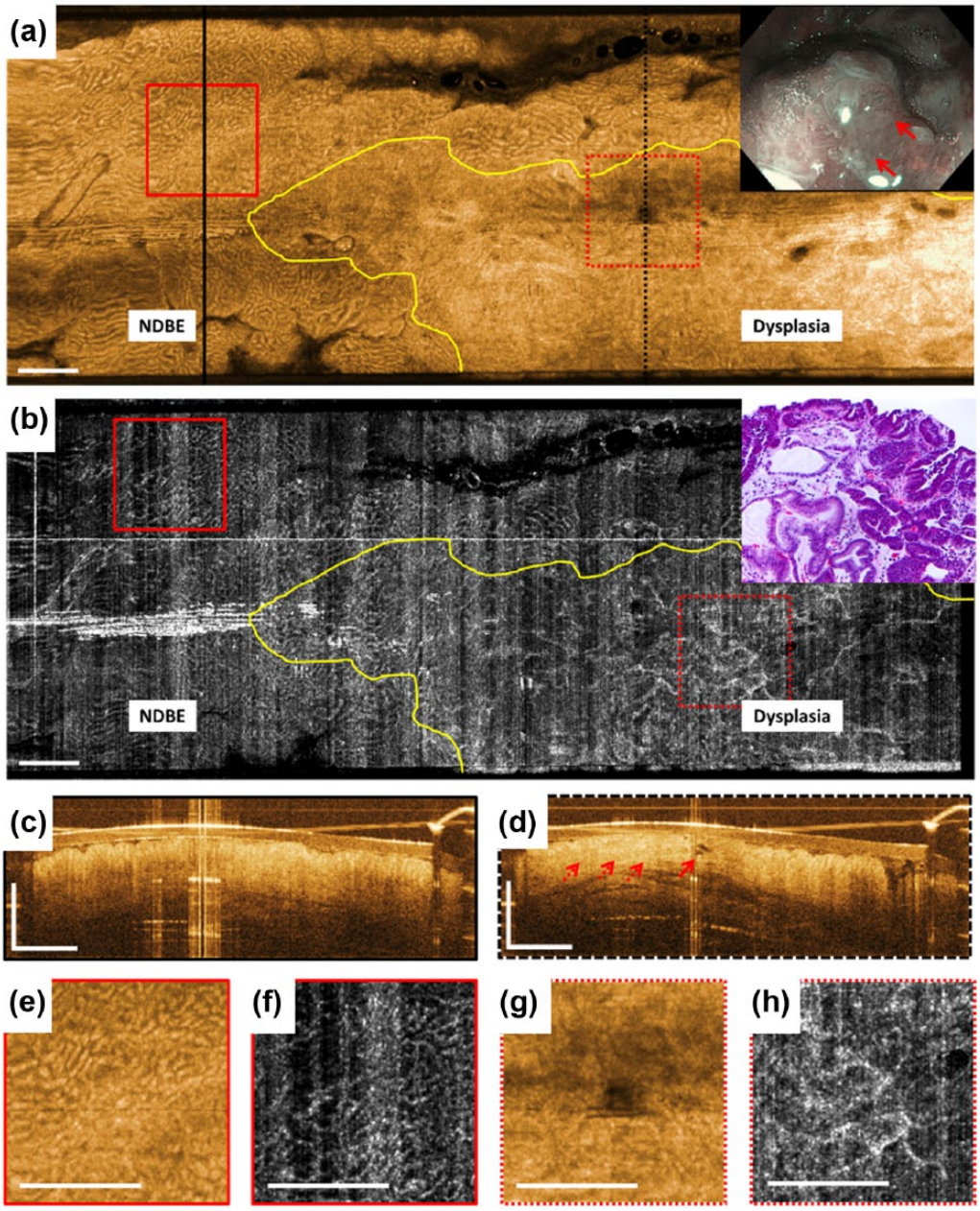

Figure 1. Optical coherence tomography (OCT), OCT angiography (OCTA), and endoscopy images acquired prior to endoscopic mucosal resection (EMR). (a) This shows an *en face* OCT image and (b) shows an *en face* OCTA image at about 250 μm below the tissue surface. Yellow lines delineate the distal and one of the transverse lateral margins of the dysplastic lesion. (c) and (d) These show cross-sectional OCT images of the areas in black lines in (a). The solid red arrow in (d) points to atypical dilated glands and the dotted red arrows show atypical glandular architecture and higher surface than subsurface signal. (e), (f), (g), and (h) These show a two times zoom over the boxed areas in (a) and (b). The inset in (a) shows the corresponding white light endoscopy/narrow band imaging image prior to EMR. The solid red arrows point to the nodular lesion. The inset in (b) shows hematoxylin and eosin stained histology of the resected specimen. Scale bars are 1 mm. NDBE, non-dysplastic Barrett's esophagus.

microvascular patterns (Figure 1b). The adjacent dysplastic lesion exhibited abnormal vessel branching. Cross-sectional OCT of the gastric/NDBE region was identified by regular vertical crypt architecture (Figure 1c). Cross-sectional OCT of the dysplastic region exhibited atypical glandular

architecture, atypical dilated glands, as well as higher surface than subsurface signal (Figure 1d). Subsequent histology of the resected EMR specimen confirmed the presence of HGD with focal intramucosal carcinoma (inset, Figure 1b).

Immediately after EMR, the resection site exhibited bleeding, debris, and cautery marks (inset, Figure 2a). The resection site was identified in the *en face* OCT image at 250 μm depth by its relatively smooth appearance caused by the cauterized tissue and lamina propria/muscularis mucosa (LP/MM) layers displaced to the surface (Figure 2a). In the *en face* OCTA image at 250 μm depth, the resection site was identified by its lack of vascular contrast (Figure 2b). A region with irregular mucosal patterns was observed between the gastric/NDBE region and the resection site, suggesting a positive lateral margin and residual dysplasia. Cross-sectional OCT of this region exhibited atypical glandular architecture, atypical dilated glands and irregular surface (Figure 2c). Cross-sectional OCT of the resection site showed cauterized tissue and the LP/MM layers on the surface as hyper-reflective layers, as well as deep ductal/lymphatic structures (dotted red arrows in Figure 2d).

WLE/NBI and OCT/OCTA images from the EMR region on follow-up endoscopy at 2-month showed a residual dysplastic lesion, confirming OCT findings of the resection site immediately following EMR (Figure 3). In the *en face* OCT image at 250 μm depth, neosquamous mucosa was identified by the relatively smooth appearance and bright OCT signal (Figure 3a), while in the *en face* OCTA image at 250 μm depth this region showed normal branching vascular appearance, characteristic of the LP layer (Figure 3b). The adjacent dysplastic lesion exhibited irregular mucosal and microvascular patterns similar to that previously described. This area was resected *via* EMR and subsequent histology of the resected specimen confirmed the presence of HGD (inset, Figure 3b). The patient subsequently underwent several EMR, cryoablation, and radiofrequency ablation procedures until complete remission of the intestinal metaplasia was achieved.

Discussion and conclusion

This case demonstrates probe-based endoscopic OCT for a comprehensive evaluation of a dysplastic lesion before and after endoscopic therapy. OCT/OCTA prior to EMR visualized the dysplastic lesion and its lateral margins. This could be particularly helpful for flat lesions where localization of dysplasia by WLE/NBI can be difficult. Immediately after EMR, when WLE/NBI visualization can be compromised by tissue distortion, electrocautery, and blood, the OCT probe allowed direct lavage over the area, and OCT/OCTA showed residual dysplasia at the distal resection margin. Confocal endomicroscopy, which generally requires intravenous contrast, is ineffective immediately after EMR because of dye leakage. Due to software limitations at the time of this study, OCTA images were not available in real time during the endoscopy, and resection under OCT/OCTA guidance was not approved under IRB protocols, so additional EMR was not performed at the time of initial treatment. However, these results suggest that OCT/OCTA can potentially play an important role in guiding endoscopic eradication therapies such as EMR to facilitate complete removal of dysplastic lesions in a single visit.

The probe-based OCT catheter used in this study[6,10] has a smaller field of view but finer transverse resolution compared with balloon- and capsule-based imaging (the probe diameter was 3.4 mm, while balloons and capsules can have 12–20 mm diameters).[4,7,11] A balloon catheter can be inflated to stabilize the esophagus and image the portions of the esophagus that are in contact with the balloon. However, there can be sampling errors where the esophagus is not in contact and a simultaneous endoscopic view of the OCT-imaged region is not possible. Tethered capsules can image large fields of view by proximally pulling back the capsule, but can also have sampling errors due to incomplete esophageal contact or nonuniform pullback.[7] The small diameter of the OCT probe allows direct assessment of the cardia and hiatal hernia under endoscopic guidance. However, its smaller field of view necessitates multiple image acquisitions to cover large regions of interest.

In interpreting the OCT/OCTA images, previously published features were used to outline regions of dysplasia.[8,12,13] Specifically, in *en face* OCT/OCTA images, regions with irregular mucosal and microvascular patterns were classified as dysplastic. In cross-sectional OCT images,

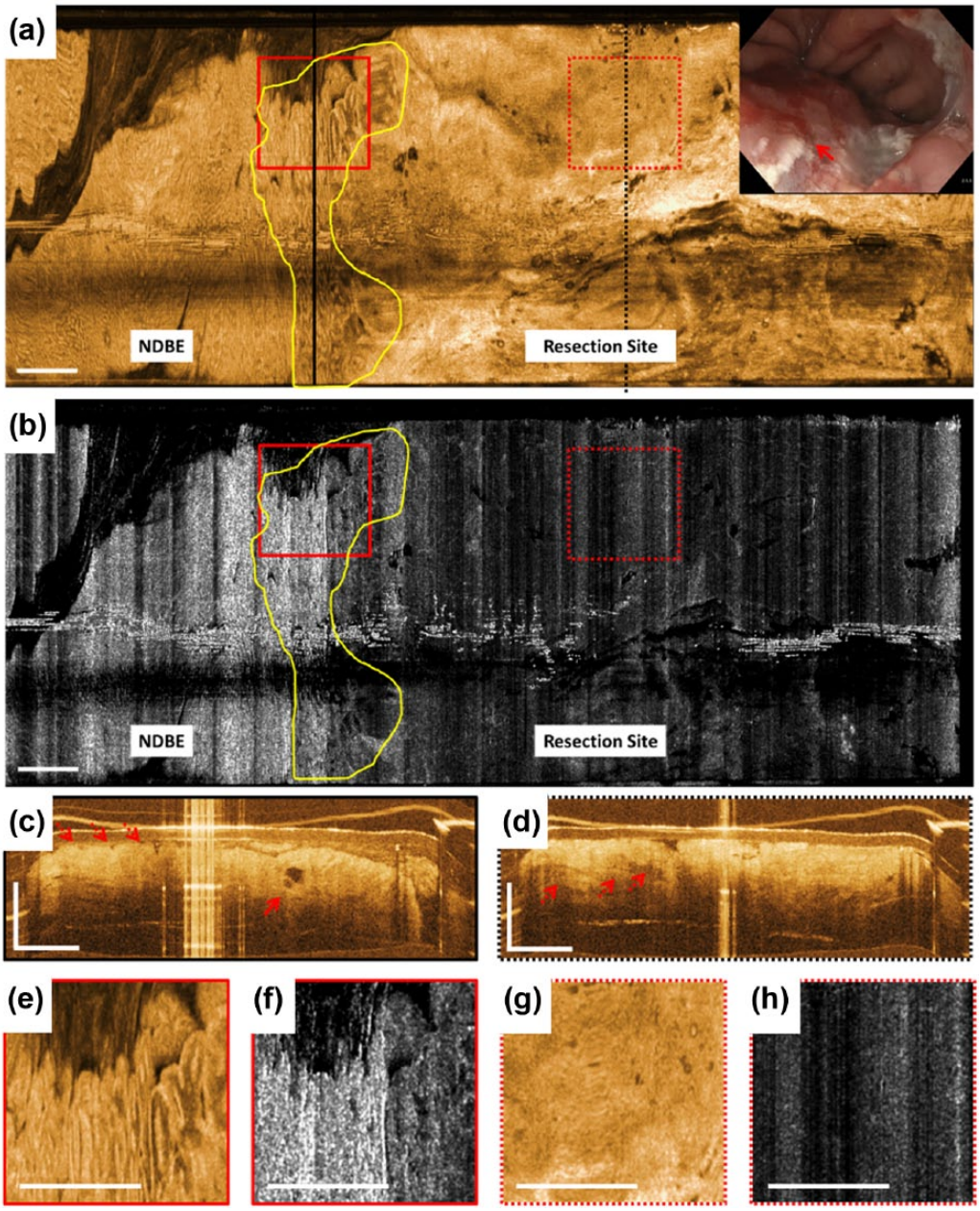

Figure 2. Optical coherence tomography (OCT), OCT angiography (OCTA), and endoscopy images acquired immediately after endoscopic mucosal resection (EMR). (a) This shows an *en face* OCT image and (b) shows an *en face* OCTA image at about 250 µm below the tissue surface. Yellow lines mark an area with irregular mucosal patterns between the gastric/non-dysplastic Barrett's esophagus (NDBE) region and the resection site suggesting a positive lateral margin and residual dysplasia. OCTA images of the gastric/NDBE region and lateral EMR margin exhibit high noise due to motion artifacts. (c) and (d) These show cross-sectional OCT images of the areas in black lines in (a). The solid red arrow in (c) points to atypical dilated glands and the dotted red arrows show atypical glandular architecture and irregular surface. The dotted red arrows in (d) show deep ductal/lymphatic structures at the resection site. (e), (f), (g), and (h) These show a two times zoom over the boxed areas in (a) and (b). The inset in (a) shows the corresponding white light endoscopy image immediately after EMR. The solid red arrow points to the resection site where endoscopic visibility is limited due to bleeding, debris, and cautery marks. Scale bars are 1 mm.

regions with atypical glandular architecture, atypical dilated and debris-filled glands, higher surface than subsurface signal, and irregular surface were classified as dysplastic. The optimal criteria for

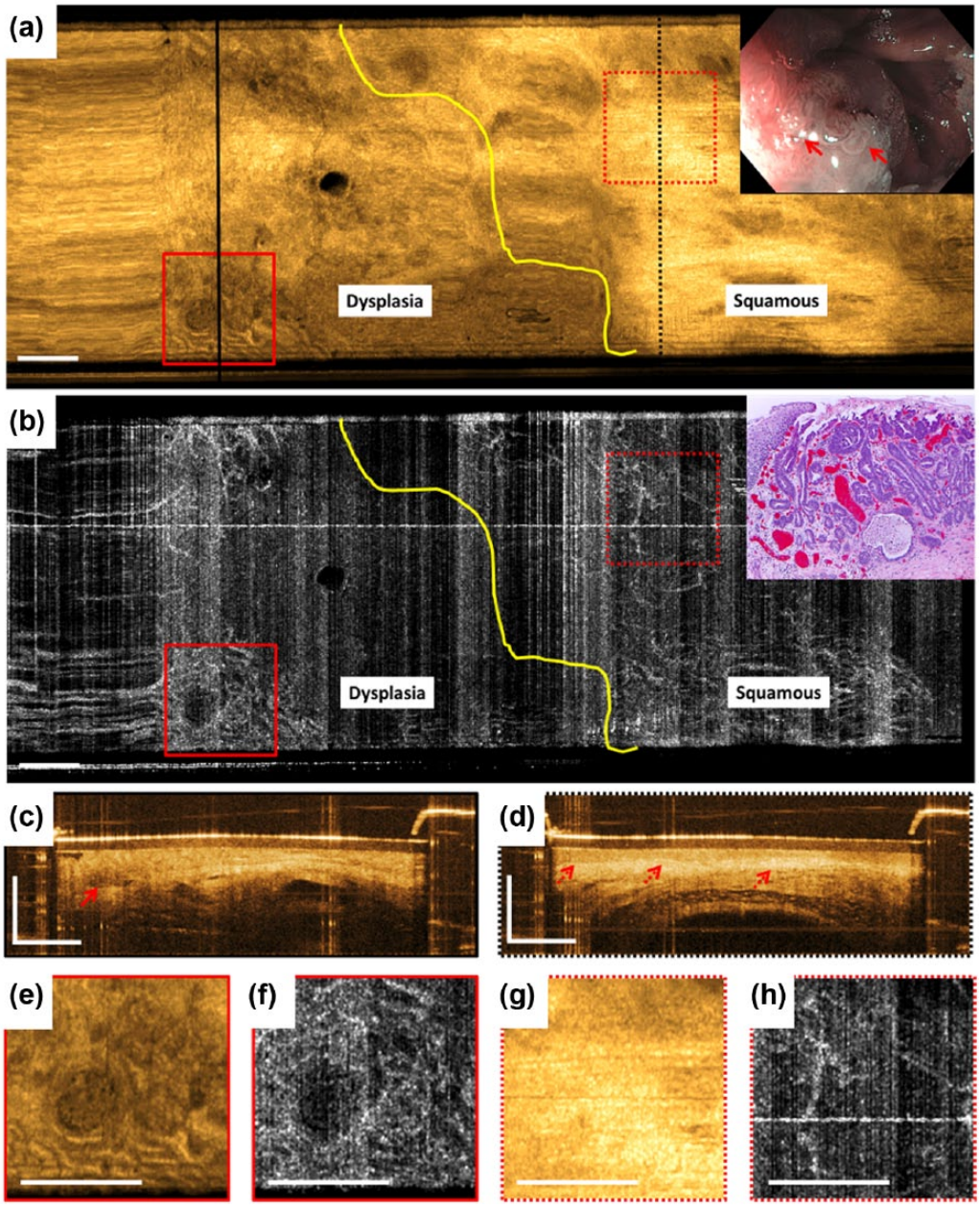

Figure 3. Optical coherence tomography (OCT), OCT angiography (OCTA), and endoscopy images acquired over the previous endoscopic mucosal resection (EMR) area at 2-month follow up. (a) This shows an *en face* OCT image and (b) shows an *en face* OCTA image at about 250 μm below the tissue surface. Yellow lines delineate the proximal lateral margin of the residual dysplastic lesion. (c) and (d) These show cross-sectional OCT images of the areas in black lines in (a). The solid red arrow in (c) points to an atypical debris-filled dilated gland. The dotted red arrows in (d) point to lamina propria/muscularis mucosa and submucosa layers underneath the homogeneous squamous epithelium layer typical of normal esophagus. (e), (f), (g), and (h) These show a two times zoom over the boxed areas in (a) and (b). The inset in (a) shows corresponding white light endoscopy/narrow band imaging image prior to EMR. The solid red arrows point to the nodular lesion at the squamocolumnar junction. The inset in (b) shows hematoxylin and eosin stained histology of the resected specimen. Scale bars are 1 mm.

identifying dysplasia with volumetric OCT are still under investigation.

In summary, probe-based OCT/OCTA provides cross-sectional and *en face* microstructural images

as well as *en face* microvascular images, which may improve diagnostic capabilities and enhance clinical utility by identifying dysplastic areas, assessing lesion margins, and evaluating regions immediately post-treatment and on follow up. Probe-based OCT/OCTA may have advantages over balloon- and capsule-based OCT and confocal endomicroscopy in certain settings.

Funding

This work was supported by facility support from the VA Boston Healthcare System, NIH grants R01-CA075289-20 (JGF and HM), R01-CA178636-04 and R01-EY011289-30 (JGF), Air Force Office of Scientific Research contracts FA9550-15-1-0473 and FA9550-12-1-0499 (JGF).

Conflict of interest statement

The authors declare that there is no conflict of interest.

References

1. Hwang JH, Konda V, Dayyeh BKA, *et al.* Endoscopic mucosal resection. *Gastrointest Endosc* 2015; 82: 215–226.
2. Mino-Kenudson M, Brugge WR, Puricelli WP, *et al.* Management of superficial Barrett's epithelium-related neoplasms by endoscopic mucosal resection: clinicopathologic analysis of 27 cases. *Am J Surg Pathol* 2005; 29: 680–686.
3. Prasad GA, Buttar NS, Wongkeesong LM, *et al.* Significance of neoplastic involvement of margins obtained by endoscopic mucosal resection in Barrett's esophagus. *Am J Gastroenterol* 2007; 102: 2380–2386.
4. Swager A, Boerwinkel D, Bruin D, *et al.* Volumetric laser endomicroscopy in Barrett's esophagus: a feasibility study on histological correlation. *Dis Esophagus* 2016; 29: 505–512.
5. Wolfsen HC, Sharma P, Wallace MB, *et al.* Safety and feasibility of volumetric laser endomicroscopy in patients with Barrett's esophagus (with videos). *Gastrointest Endosc* 2015; 82: 631–640.
6. Tsai TH, Ahsen OO, Lee HC, *et al.* Endoscopic optical coherence angiography enables 3-dimensional visualization of subsurface microvasculature. *Gastroenterology* 2014; 147: 1219–1221.
7. Liang K, Ahsen OO, Lee H-C, *et al.* Volumetric mapping of Barrett's esophagus and dysplasia with en face optical coherence tomography tethered capsule. *Am J Gastroenterol* 2016; 111: 1664.
8. Lee H-C, Ahsen OO, Liang K, *et al.* Endoscopic optical coherence tomography angiography microvascular features associated with dysplasia in Barrett's esophagus: a pilot study (with video). *Gastrointest Endosc* 2017; 86: 476–484.
9. Sharma P, Dent J, Armstrong D, *et al.* The development and validation of an endoscopic grading system for Barrett's esophagus: the Prague C & M criteria. *Gastroenterology* 2006; 131: 1392–1399.
10. Tsai T-H, Lee H-C, Ahsen OO, *et al.* Ultrahigh speed endoscopic optical coherence tomography for gastroenterology. *Biomed Opt Express* 2014; 5: 4387–4404.
11. Lee H-C, Ahsen OO, Liang K, *et al.* Circumferential optical coherence tomography angiography imaging of the swine esophagus using a micromotor balloon catheter. *Biomed Opt Express* 2016; 7: 2927–2942.
12. Leggett CL, Gorospe EC, Chan DK, *et al.* Comparative diagnostic performance of volumetric laser endomicroscopy and confocal laser endomicroscopy in the detection of dysplasia associated with Barrett's esophagus. *Gastrointest Endosc* 2016; 83: 880–888.e2.
13. Sharma P, Bergman JJ, Goda K, *et al.* Development and validation of a classification system to identify high-grade dysplasia and esophageal adenocarcinoma in Barrett's esophagus using narrow-band imaging. *Gastroenterology* 2016; 150: 591–598.